Supplementary Information for
Negative-to-Positive Tunnel Magnetoresistance in van der Waals $Fe_3GeTe_2/Cr_2Ge_2Te_6/Fe_3GeTe_2$ Junctions

Zi-Ao Wang(王子奥)[1,2], Xiaomin Zhang(张晓敏)[1,2], Wenkai Zhu(朱文凯)[1], Faguang Yan(闫法光)[1], Pengfei Liu(刘鹏飞)[1], Zhe Yuan(袁喆)[3] and Kaiyou Wang(王开友)[1,2]*

[1]State Key Laboratory of Superlattices and Microstructures, Institute of Semiconductors, Chinese Academy of Sciences, Beijing 100083, China

[2]Center of Materials Science and Optoelectronics Engineering, University of Chinese Academy of Sciences, Beijing 100049, China

[3]Center for Advanced Quantum Studies and Department of Physics, Beijing Normal University, Beijing 100875, China

*Corresponding author. Email: kywang@semi.ac.cn

Section 1: Methods

Device fabrication. We pre-patterned Cr/Au (10/25 nm) electrodes on a 300-nm-thick SiO_2/Si substrate by photolithography, sputter deposition, and lift-off. The high-quality van der Waals bulk single-crystal FGT and CGT (both from HQ Graphene) were mechanically exfoliated into few-layer flakes inside a nitrogen-filled glove box. We used the polydimethylsiloxane (PDMS) dry transfer method to transfer the FGT and CGT flakes sequentially onto the electrode-prepared substrate to form the FGT/CGT/FGT MTJ. Then, we used a piece of hBN with a thickness of ~ 40-50 nm to encapsulate the device for protection. Finally, the device was annealed at 393 K in the glove box to eliminate possible air gaps and ensure a tight fit between the flakes.

Characterizations. The samples were mounted in a cryogenic probe station in an ultra-high vacuum environment (Lake Shore Cryotronics, Inc.) with a base temperature of 10 K and a magnetic field of 2.25 T along the out-of-plane direction. The electrical and magneto-transport measurements were performed using a Keithley

Model 2602B source meter in conjunction with a Keithley Model 2182A nanovoltmeter. The thickness of the CGT flake was determined by atomic force microscopy (AFM) (Bruker Multimode 8).

First-principles calculations. First-principles calculations based on density functional theory are carried out using the projected augmented-wave method implemented in the Vienna Ab Initio Simulation Package (VASP).[1,2] The general gradient approximation is employed in conjunction with the Perdew-Burke-Ernzerhof type exchange-correlation functional. The wave functions are expanded in a plane-wave basis with an energy cutoff of 500 eV. The electronic structure of bulk FGT is calculated self-consistently with its lattice constant a = 4.044 Å and c = 17.201 Å. To calculate the density of states, we use 21×21×5 k points to sample the Brillouin zone. The influence of a finite bias on the FGT electrode is modeled by shifting the Fermi energy rigidly corresponding to its voltage.[3]

Section 2: The two-state magnetoresistance in FGT/CGT/FGT MTJs

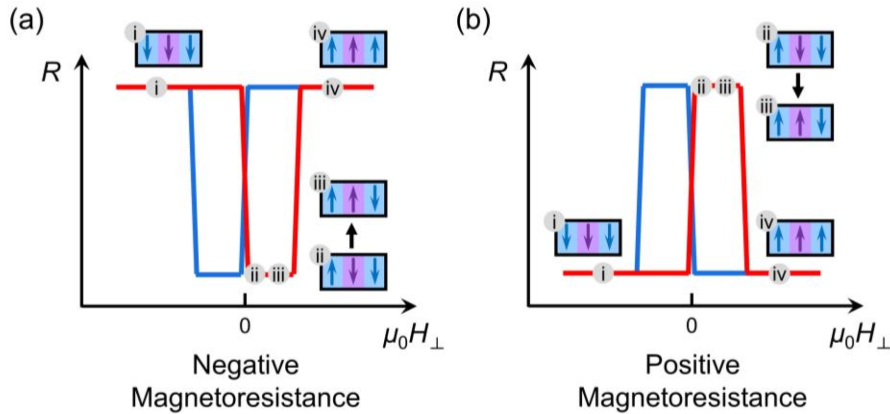

Fig. S1. Schematic diagram for magnetization alignments of FGT/CGT/FGT MTJs of negative (a) and positive (b) magnetoresistance effects as the magnetic field sweeping. The blue and purple arrows represent the magnetization directions of FGT and CGT, respectively. The red (blue) curves present the magnetic field sweeping from negative (positive) to positive (negative).

According the pervious report and our previous work, CGT exhibits a small coercivity of ~ 3 mT.[4,5] We take the positive bias voltage as an example to discuss

the magnetization alignments in FGT/CGT/FGT MTJs in two cases: negative and positive magnetoresistance effects, as shown in Figs. S1(a) and (b), respectively. Under the positive bias voltage (the electric field pointing toward the bottom FGT electrode), the charge transfer at bottom CGT/FGT interface will be enhanced but the one at the top FGT/CGT interface will be suppressed, leading to the H_C of bottom FGT electrode reduced to 0 mT. Taking the case of negative magnetoresistance effect as an example [Fig. S1(a)], when the magnetic field sweeps from negative to zero, the bottom FGT electrode switches first (↑↓↓) and then immediately the CGT layer switches (↑↑↓), followed by a jump back to the high-resistance state (↑↑↑) at the large positive magnetic field. For the case of positive magnetoresistance, the magnetization alignments of FGT/CGT/FGT MTJs are similar except that the parallel magnetic configuration (↓↓↓ or ↑↑↑) corresponds to the low-resistance state, as shown in Fig. S1(b). The resistance curve exhibits a similar jump down and up when the magnetic field sweeps back to negative (blue curve). Therefore, the magnetoresistance of FGT/CGT/FGT MTJs only have two states. Our results suggest that the magnetization alignment of CGT have not obvious influence on the magnetoresistance of FGT/CGT/FGT MTJs.

Section 3: The thickness of CGT interlayer in device 2

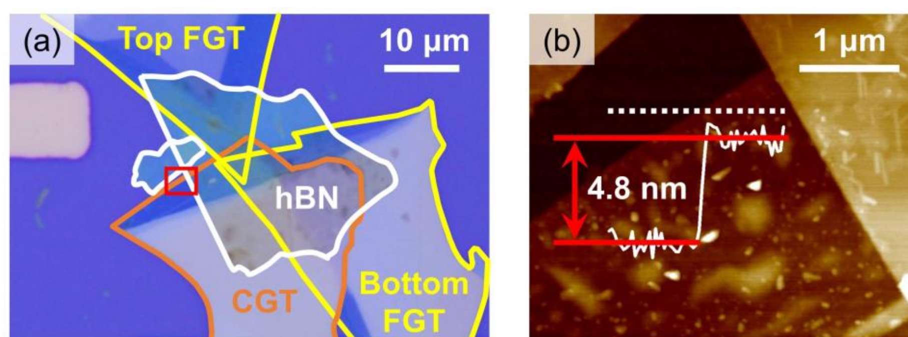

Fig. S2. (a) The optical image of device 2 with hBN encapsulation. The yellow lines outline the FGT electrodes; the orange line outlines the CGT interlayer; the white lines outline the hBN covering layer. (b) The AFM image of device 2. Height profile of CGT interlayer along the white dashed line in (b). The area shown in the (b) is marked out in the optical image (a) by the small red square.

We performed the AFM measurement for FGT/CGT/FGT MTJs and show device 2 as an example in Fig. S2, where the thickness of CGT interlayer is 4.8 nm.

Section 4: The temperature dependent *J*-*V* curves of device 2

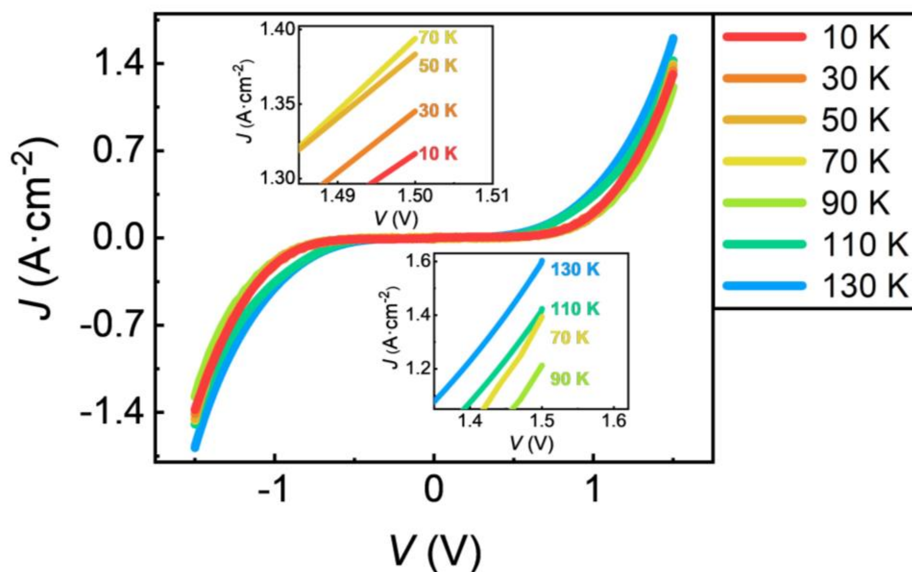

Fig. S3. The *J*-*V* curves for the FGT/CGT/FGT MTJ (device 2) at different temperatures (*T*). The Insets are the zoomed views of *J*-*V* curves with *T* ranging from 10 K to 70 K (top panel) and *J*-*V* curves with *T* ranging from 70 K to 130 K (bottom panel).

The *J*-*V* curves for device 2 with *T* ranging from 10 K to 130 K are shown in Fig. S3. As the temperature raises from 10 K to 70 K, the current density of the FGT/CGT/FGT MTJ increases gradually but the magnitude of change is small. When 70 K $< T \leq$ 90 K, the weakened metallization of interfacial CGT layer makes the resistance increase, leading to the current density decreasing significantly. When T > 90 K, the current density increases monotonically with increasing temperature, consistent with the temperature dependence of the tunneling current in the tunnel junction.[6]

Section 5: Extended data about a CGT/FGT bilayer

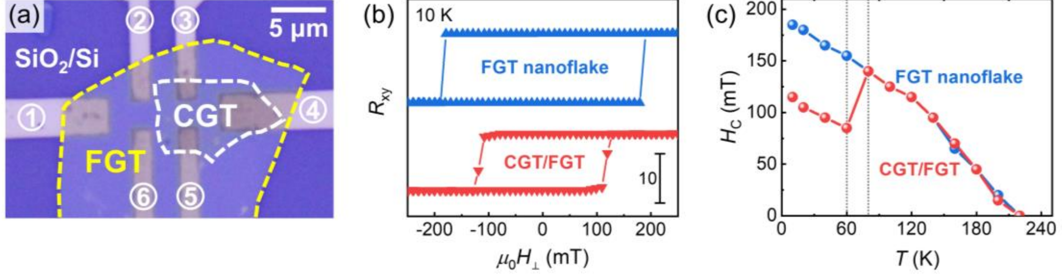

Fig. S4. (a) Optical image of the CGT/FGT bilayer. The yellow and the white line outline the edges of FGT and CGT flakes, respectively. (b) Out-of-plane magnetic-field-dependent Hall resistances (R_{xy}) of the individual FGT device (top panel, measuring with electrodes No.1, No.2, No.4 and No.6) and CGT/FGT bilayer (bottom panel, measuring with electrodes No.1, No.3, No.4 and No.5) at 10 K. (c) Extracted H_C of the CGT/FGT bilayer and individual FGT device at different temperatures.

A CGT/FGT bilayer was fabricated by mechanical exfoliation from the same bulk single-crystal FGT and CGT as FGT/CGT/FGT MTJs and dry transfer method, where the FGT is only half covered by CGT, as shown in Fig. S4(a). We performed the anomalous Hall effect measurements for this device under different temperature and summarized the temperature-dependent H_C of CGT/FGT bilayer and FGT nanoflake is in Fig. S4(c). When $T \leq 60$ K, due the directional charge transfer from FGT to CGT,[4] the H_C of FGT in CGT/FGT bilayer is suppressed remarkably compared with that of FGT nanoflake [Figs. S4(b) and (c)]. When the temperature is near $T_C \sim 65$ K of CGT, the band structure change of the CGT leads to a change in the amount of transferred charge, thus the magnetic properties of CGT/FGT bilayer will be different. Therefore, the reduction of the H_C gradually disappears at 60 K < T < 80 K shown in Fig. S4(c) indicates that T_C of CGT is not increased by neighboring to FGT.

References

[1] Kresse G and Furthmüller J 1996 *Phys. Rev. B* 54 11169

[2] Kresse G and Joubert D 1999 *Phys. Rev. B* 59 1758

[3] Sharma M, Wang S X and Nickel J H 1999 *Phys. Rev. Lett.* 82 616

[4] Wang Z A, Xue W, Yan F, Zhu W, Liu Y, Zhang X, Wei Z, Chang K, Yuan Z and Wang K 2023 *Nano Lett.* 23 710

[5] Carteaux V, Brunet D, Ouvrard G and Andre G 1995 *J. Phys. Condens. Matter* 7 69

[6] Cobas E, Friedman A L, van't Erve O M J, Robinson J T and Jonker B T 2012 *Nano Lett.* 12 3000